Argonne NATIONAL LABORATORY

ANL-GenIV-079

Feasibility Study for Use of the Natural Convection Shutdown Heat Removal Test Facility (NSTF) for VHTR Water-Cooled RCCS Shutdown

Nuclear Engineering Division

About Argonne National Laboratory

Argonne is a U.S. Department of Energy laboratory managed by UChicago Argonne, LLC under contract DE-AC02-06CH11357. The Laboratory's main facility is outside Chicago, at 9700 South Cass Avenue, Argonne, Illinois 60439. For information about Argonne, see www.anl.gov.

Availability of This Report

This report is available, at no cost, at http://www.osti.gov/bridge. It is also available on paper to the U.S. Department of Energy and its contractors, for a processing fee, from:

U.S. Department of Energy
Office of Scientific and Technical Information
P.O. Box 62
Oak Ridge, TN 37831-0062
phone (865) 576-8401
fax (865) 576-5728
reports@adonis.osti.gov

ANL-GenIV-079

Feasibility Study for Use of the Natural Convection Shutdown Heat Removal Test Facility (NSTF) for Initial VHTR Water-Cooled RCCS Shutdown

by
C.P. Tzanos, M.T. Farmer
Nuclear Engineering Division, Argonne National Laboratory

September 2006

List of Figures

List of Tables

Nomenclature

A = flow area
A_α = flow area in the annulus
A_{in} = flow area of the pipe feeding the tank
A_{out} = flow area of pipe leading out of the tank
C_p = fluid specific heat
D = hydraulic diameter
D_{Ip} = diameter of inner tube
E = enthalpy
E_r = reference enthalpy
f = friction factor
g = acceleration of gravity
H = height
h_a = heat transfer coefficient in the annulus
h_I = heat transfer coefficient in the inner tube
K = loss coefficient
k = conductivity
L = length
L_a = vertical length of the hot leg above the heated section
L_c = vertical length of the cold leg before it enters the heated section
L_h = length of heated section
P_e = perimeter of the ellipsoidal tube
δp_f = frictional pressure drop
P_I = perimeter of the inner tube
p_{in} = pressure at the top of a tank
δp_ℓ = other pressure losses
p_{out} = pressure at the top of the hot leg (exit of return line)
Δp = $p_{in} - p_{out}$
ΔP = dimensionless pressure = $\dfrac{\Delta p}{\rho_o U_r^2}$
R = radius
T_c = temperature of the cold wall
T_e = temperature of water in the annulus
T_I = temperature of water in the inner tube
T_h = reactor vessel temperature
T_{se} = temperature of the ellipsoidal tube
T_{sI} = temperature of the inner tube

T_o = reference temperature

T_{out} = water temperature at the outlet of the heated section of the RCCS

t = time

U = velocity

$u^* = \frac{\mu}{\rho H}$ = reference velocity in air-cavity

V = velocity component in the horizontal direction (Y)

W = velocity component in the vertical direction (Z)

x = vapor quality

Y, Z = Cartesian coordinates

Greek Symbols

α = void fraction

α^* = thermal diffusivity

β = volumetric coefficient of thermal expansion

δ = structure thickness

ε = emissivity

μ = dynamic viscosity

θ = non-dimensional temperature

θ_I = non-dimensional temperature of water in the inner tube

θ_{sI} = non-dimensional temperature of inner tube (structure)

θ_{se} = non-dimensional temperature of water in the annulus between the RCCS tubes

ρ = water density

ρ_c = water density in the cold leg before it enters the heated section

$\Delta\rho$ = $\rho - \rho_g$

σ = Stefan-Boltzmann constant

σ_s = surface tension

τ = non-dimensional transport time

τ^* = non-dimensional conduction time

Subscripts

b = boiling

bv = boiling vertical section

c = cold

d = down

g = vapor

h = hot

I = inner

ℓ = liquid

m = mean

o = outer

out = tank outlet
p = pipe
r = reference value
s = structure
out = tank outlet
t = tank
TP = two-phase
x = exit
w = water

Similarity Groups

$$B_i = \frac{h\delta}{k}, \quad \text{Biot number}$$

$$N_c = \frac{A_c h_{cav}}{A_o \rho C_p U_o}, \quad \text{Cavity convective number}$$

$$N_r = \frac{A_{rad}\varepsilon\sigma T_o^4}{U_o A_o \rho_o C_p \left(T_r - T_o\right)}, \quad \text{Cavity radiation number}$$

$$N_d = \frac{V_{gj}}{U_o}, \quad \text{Drift flux number}$$

$$F_r = \frac{U_r^2}{gL_r}, \quad \text{Froude number}$$

$$F = \frac{f\ell}{d} + K, \quad \text{Friction number}$$

$$N_{fi} = \left(\frac{fl}{d}\right)_i \left[\frac{1 + x\left(\Delta\rho/\rho_g\right)}{\left(1 + x\,\Delta\mu/\mu_g\right)^{0.25}}\right]\left(\frac{A_o}{A_i}\right)^2, \quad \text{Friction number (two-phase flow)}$$

$$N_o = K_i\left[1 + x^{3/2}\left(\Delta\rho/\rho_g\right)\right]\left(\frac{A_o}{A_i}\right)^2, \quad \text{Orifice number}$$

$$\mathrm{Pr} = \frac{C_p\mu}{k}, \quad \text{Prandtl number}$$

$$R\alpha = \frac{C_p\rho^2 g\beta\left(T_h - T_c\right)H^3}{\mu k}, \quad \text{Rayleigh number}$$

$$Ri = \frac{g\beta\left(T_r - T_o\right)L_r}{U_r^2},$$ Richardson number

$$St_I = \frac{4h_I L_r}{\rho C_p U_r D_{ip}},$$ Stanton number (inner tube)

$$St_e = \frac{P_e h_\alpha L_r}{\rho C_p U_r A_\alpha},$$ Stanton number (annulus, outer wall)

$$St_\alpha = \frac{P_I h_I L_r}{\rho C_p U_r A_\alpha},$$ Stanton number (annulus, inner wall)

$$N_t = \frac{T_r - T_o}{T_o},$$ Temperature ratio number

$$T^* = \frac{\alpha}{\delta^2}\frac{L_r}{U_r},$$ Time Ratio number

1.0 Introduction and Summary

1.1 Background

Defense-in-depth, containment and emergency planning are all part of the safety strategy to assure the protection of the public in the determination of the siting source term. The Reactor Cavity Cooling System (RCCS) is a system which is important to the passive safety case being incorporated in this overall safety strategy. The RCCS will be one of the new safety systems specifically designed for the next generation of nuclear power plants being developed under the auspices of the DOE GENIV program. In particular, it is being developed and being incorporated into the proposed reactor and plant designs for the Very High Temperature Reactor (VHTR). The VHTR is a helium gas-cooled nuclear plant with a thermal-spectrum reactor. The RCCS forms a passive heat sink external to the reactor, and is located within the reactor cavity/silo surrounding the metal vessel. During emergency accident conditions when all a/c power is lost, natural convection of the RCCS coolant removes the heat radiated or naturally convected from the metal vessel wall to the inner boundary of the RCCS facing the vessel. This will be a First-of-A-Kind (FOAK) passive safety system for core decay heat removal when the FOAK VHTR is built.

But, it should be noted that the RCCS had a predecessor in the Reactor Vessel Auxiliary Cooling System (RVACS) developed by the Advanced Liquid Metal Reactor (ALMR) program. This was a passive safety system which provided for the removal of core decay heat in an emergency mode through the cooling of the reactor vessel wall by the natural convection of air. The air-cooled version of the RCCS for the VHTR is very similar to the RVACS that has been proposed for the General Electric PRISM ALMR design. The design and safety analysis of the RVACS are based on extensive analytical and experimental work performed at ANL. The Natural Convection Shutdown Heat Removal Test Facility (NSTF) at ANL was built to provide a full scale simulation of the air-side of the PRISM RVACS system, and to provide experimental support for the design and analysis of this system. In FY05, work was performed to demonstrate that the NSTF facility can be used to generate experimental data to validate CFD and systems codes for the analysis of an air-cooled RCCS for the VHTR and to support the design and safety analysis of this RCCS type [1-3]. More specifically, the objectives were to: (a) develop the scaling relations to be used in modifying the existing NSTF facility into a scaled model of the VHTR air-cooled RCCS; and (b) provide a summary of the NSTF modifications needed to conduct scaled simulations of the RCCS. The main conclusion of the FY05 study was that these air-cooling NSTF simulations will generate experimental data suitable for code validation and RCCS design validation and optimization.

However, there exists another design option for the VHTR RCCS and this is one which utilizes water-cooling in place of air cooling. In FY06, the objective for the effort is to perform a NSTF feasibility study similar to that conducted in FY05 but to focus on the water-cooled RCCS instead of the air-cooled RCCS. Although a specific design has not yet been selected for the VHTR, the PBMR water-based RCCS is used as a planning

basis for the purposes of this study. This design is mature enough to allow the development of an appropriately scaled experimental facility. In FY05, the air-cooled RCCS of the GT MHR was used as the planning basis. Figure 1 taken from [4] shows a possible design for the water-cooled RCCS of PBMR. The RCCS standpipe array is shown. These surround the reactor pressure vessel (RPV). The vessel with the surrounding RCCS standpipe array is then centered in the reactor cavity/silo/citadel which is poured in concrete. Figure 2 shows an axial elevation while Fig. 3 shows a potential configuration for he cross-section of the RCCS standpipes. The water cooled RCCS standpipes consists of ~60 oval tubes. Each oval tube is made of structural steel with a cross-section of ~0.25 m x ~1.0 m. The major heat transfer section is ~20 m in height but there is ~40 m to the top of the water storage tanks. These water storage tanks provide the boil-down passive heat inventory during the emergency decay heat removal mode. Upon total loss of a/c power, natural convection water flow starts. The water in the tanks is at ~30°C. It enters the manifolds from the tanks, where upon it distributes to the downcomers inside the oval tubes. It then flows up through the RCCS tubes and returns to the tanks. Under normal operation, forced convection heat exchangers provide cooled water to the tanks. Evaporation occurs if tank cooling is lost.

To reiterate, the objectives of the FY06 work are to demonstrate that the NSTF facility can be used to generate experimental data to validate CFD and systems codes for the analysis of the water-cooled RCCS for the VHTR, and to support the design and safety analysis of this type of RCCS. More specifically, the objectives are to: (a) develop the scaling relations to be used in modifying the existing NSTF facility into a scaled model of the VHTR water-cooled RCCS; and (b) provide a summary of the NSTF modifications needed to conduct scaled simulations of the RCCS. These simulations will generate experimental data for code validation and RCCS design validation and optimization.

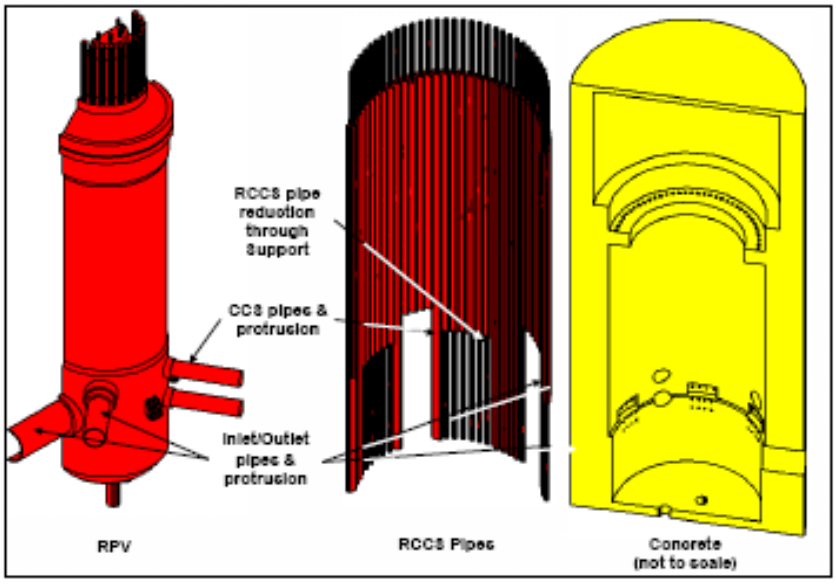

Fig. 1. Exploded View of the Main Components in the PBMR Citadel

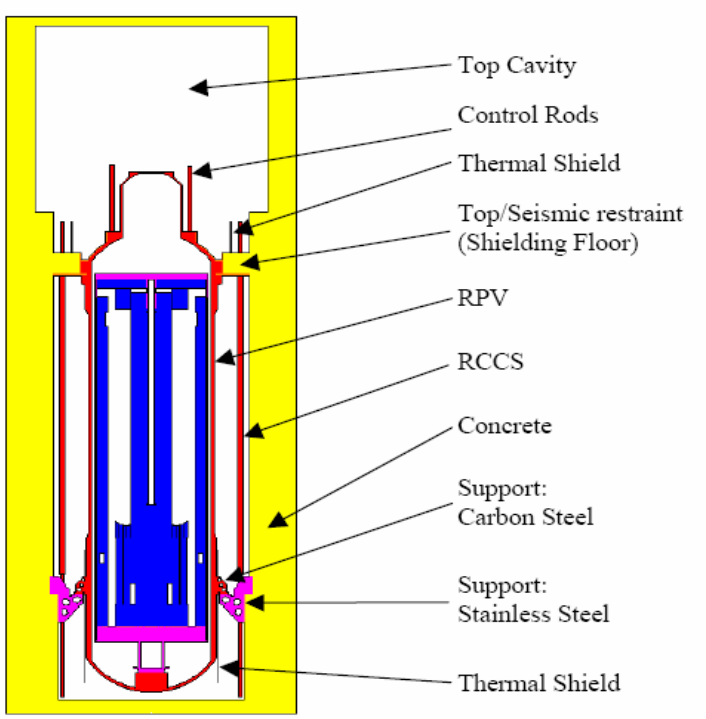

Fig. 2 PBMR Citadel Axial Elevation

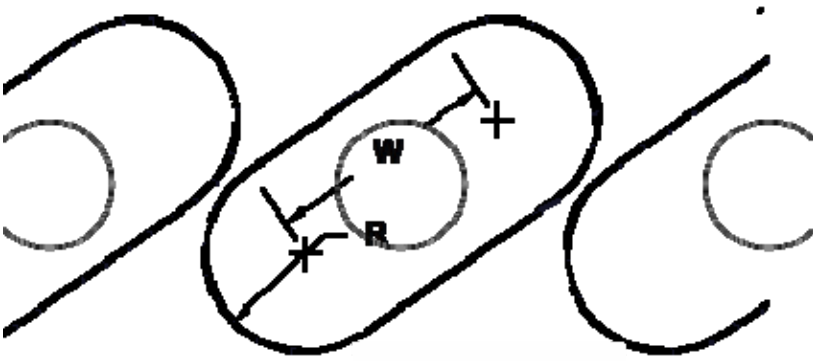

Fig. 3 PBMR RCCS Standpipe Cross-section

1.2 Summary

In summary, a scaling analysis of a water-cooled RCCS system was performed based on generic information on the RCCS design of PBMR. The analysis demonstrates that the water-cooled RCCS can be simulated at the ANL NSTF facility at a prototypic scale in the lateral direction and about half scale in the vertical direction. Because, by necessity, the scaling is based on a number of approximations, and because no analytical information is available on the performance of a reference water-cooled RCCS, the scaling analysis presented here needs to be "validated" by analysis of the steady state and

transient performance of a reference water-cooled RCCS design. The analysis of the RCCS performance by CFD and system codes presents a number of challenges including: strong 3-D effects in the cavity and the RCCS tubes; simulation of turbulence in flows characterized by natural circulation, high Rayleigh numbers and low Reynolds numbers; validity of heat transfer correlations for system codes for heat transfer in the cavity and the annulus of the RCCS tubes; the potential of nucleate boiling in the tubes; water flashing in the upper section of the RCCS return line (during limiting transient); and two-phase flow phenomena in the water tanks. The limited simulation of heat transfer in cavities presented in Section 4.0, strongly underscores the need of experimental work to validate CFD codes, and heat transfer correlations for system codes, and to support the analysis and design of the RCCS.

Based on the conclusions of the scaling analysis, a schematic that illustrates key attributes of the experiment system is shown in Fig. 4. This system contains the same physical elements as the PBMR RCCS, plus additional equipment to facilitate data gathering to support code validation. In particular, the prototype consists of a series of oval standpipes surrounding the reactor vessel to provide cooling of the reactor cavity during both normal and off-normal operating conditions. The standpipes are headered (in groups of four in the prototype) to water supply (header) tanks that are situated well above the reactor vessel to facilitate natural convection cooling during a loss of forced flow event. During normal operations, the water is pumped from a heat sink located outside the containment to the headered inlets to the standpipes. The water is then delivered to each standpipe through a centrally located downcomer that passes the coolant to the bottom of each pipe. The water then turns 180˚ and rises up through the annular gap while extracting heat from the reactor cavity due to a combination of natural convection and radiation across the gap between the reactor vessel and standpipes. The water exits the standpipes at the top where it is headered (again in groups of four) into a return line that passes the coolant to the top of the header tank. Coolant is drawn from each tank through a fitting located near the top of the tank where it flows to the heat rejection system located outside the containment. This completes the flow circuit for normal operations.

During off-normal conditions, forced convection water cooling in the RCCS is presumed to be lost, as well as the ultimate heat sink outside the containment. In this case, water is passively drawn from an open line located at the bottom of the header tank. This line is orificed so that flow bypass during normal operations is small, yet the line is large enough to provide adequate flow during passive operations to remove decay heat while maintaining acceptable fuel temperatures. In the passive operating mode, water flows by natural convection from the bottom of the supply tank to the standpipes, and returns through the normal pathway to the top of the tanks. After the water reaches saturation and boiling commences, steam will pass through the top of the tanks and be vented to atmosphere. In the experiment system shown in Fig. 4, a steam condensation and collection system is included to quantify the boiling rate, thereby providing additional validation data. This system does not exist in the prototype.

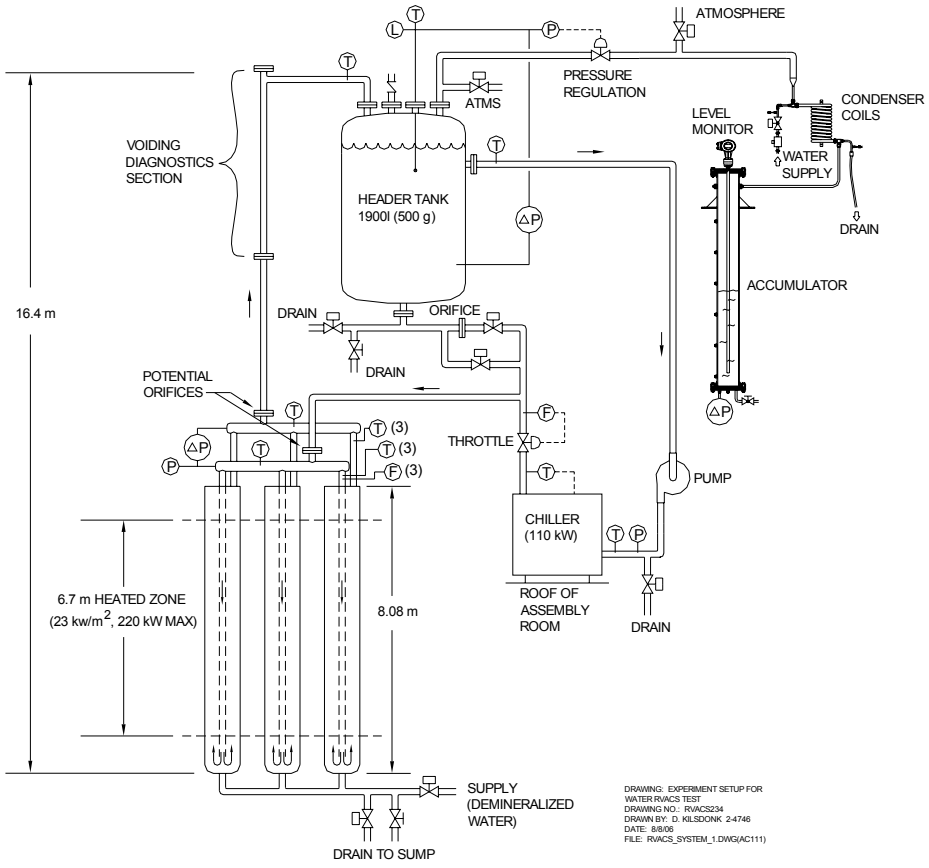

Fig. 4. Sketch of NSTF System Modifications for Water-Based RCCS Testing

The first part of the report presents the non-dimensional conservation equations describing the response of the water-based RCCS during steady-state and transient operations. These equations are used to develop similarity relationships that define a scaling of the NSTF that minimizes distortions between scaled experiments and protoype operation. Then, some limited simulations of heat transfer in cavities are presented that strongly underscore the need of experimental work to validate CFD codes, and heat transfer correlations for system codes, and to support the analysis and design of the RCCS. Finally, a summary is provided of the NSTF modifications needed to conduct scaled simulations of the RCCS.

2.0 Non-dimensional Conservation Equations

In this section, simplified one-dimensional conservation equations for mass, energy and momentum are presented for the RCCS loop, and these equation are properly non-dimensionalized to determine the non-dimensional groups that govern the similarity between the prototype RCCS and scaled models of the prototype. For the reactor cavity, the assumption is made that the arrangement of the RCCS tubes in the cavity is such that the cavity can be approximated by a simple two-dimensional rectangular cavity with vertical hot and cold walls. For the derivation of scaling ratios, the cavity is represented

as a radiating wall (reactor vessel) and a convective boundary condition on the outer surface of the RCCS tubes.

2.1 Steady State

The integral momentum equation in the water side of the RCCS can be written

$$p_{in} + \rho_c g L_a + \int_0^{L_h} \left(\rho g dL\right)_d = p_{out} + \int_0^{L_h} \left(\rho g dL\right)_u + \rho_h g L_a + \delta p_f + \delta p_\ell \tag{1}$$

The integral on the left side of Eq. (1) is the gravitational head of the cold leg in the heated section, and the integral on the right side is the gravitational head of the hot leg in the same section. The frictional pressure drop in the i th section is

$$\delta p_{f,i} = \frac{1}{2D_i} f_i \rho_i U_i^2 L_i \tag{2}$$

The form pressure losses in the i th section of the loop are

$$\delta p_{\ell,i} = \frac{1}{2} K_i \rho_i U_i^2 \tag{3}$$

where K_i is the pressure loss coefficient in the i th section.

In the sections where the density varies with the temperature, the Boussinesq approximation gives

$$\rho = \rho_o \left[1 - \beta\left(T - T_o\right)\right] \tag{4}$$

where

ρ_o = reference density
β = volumetric coefficient of thermal expansion
T_o = reference temperature

The conservation equations describing the RCCS system are non-dimensionalized using non-dimensional variables as summarized in Table 1. A non-dimensional temperature θ is defined in terms of a characteristic temperature rise, $T_r - T_o$, as

$$\theta = \frac{T - T_o}{T_r - T_o} \tag{5}$$

Then, Eq. (4) gives

$$\rho = \rho_o - \rho_o \beta \theta \left(T_r - T_o \right) \tag{6}$$

For $p_{in} = p_{out}$, substitution of Eqs. (6), (2) and (3) into Eq. (1) yields.

$$\begin{aligned} &-\rho_o g \beta \left(T_r - T_o \right) \theta_c L_a - \rho_o g \beta \left(T_r - T_o \right) \int_0^{L_h} \left(\theta dL \right)_d \\ &= -\rho_o g \beta \left(T_r - T_o \right) \int_0^{L_h} \left(\theta dL \right)_u - \rho_o g \beta \left(T_r - T_o \right) \theta_a L_a + \frac{1}{2} \sum_i \frac{f_i \rho_i U_i^2 L_i}{D_i} + \frac{1}{2} \sum_i K_i \rho_i U_i^2 \end{aligned} \tag{7}$$

Using a characteristic velocity U_r and a characteristic length L_r, and noting that the Richardson number Ri is

$$Ri = \frac{g \beta \left(T_r - T_o \right) L_r}{U_r^2} \tag{8}$$

then division of Eq. (7) by $\rho_0 U_r^2$ gives

Table 1. Non-dimensional Variables

z = Z/H	Vertical Distance
y = Y/H	Horizontal Distance
$\ell = L / L_r$	Length
$d = D / L_r$	Diameter
$E_m^* = E_m / E_r$	Mixture Enthalpy
$\Delta E_{fg}^* = \Delta E_{fg} / E_r$	Latent Heat of Vaporization
$u_m = U_m / U_r$	Mixture Velocity
$u = U / U$	Velocity (1-D Flow)
$\Delta P = \Delta p / \left(\rho U_r^2 \right)$	Pressure Drop
$V = V / u^*$	Horizontal Velocity in Cavity
$V_{gj}^* = V_{gj} / U_r$	Vapor Drift Velocity
$W = W / u^*$	Vertical Velocity in Cavity
$\theta = \left(T - T_o \right) / \left(T_r - T_o \right)$	Temperature
$\tau = U_r t / L_r$	Transport Time
$\tau^* = t \alpha^* / \delta^2$	Conduction Time
$\rho_m^* = \rho_m / \rho$	Mixture Density
$\rho_g^* = \rho_g / \rho$	Vapor Density
$\rho_\ell^* = \rho_\ell / \rho$	Fluid Density

$$Ri\left[-\int_0^{\ell_h}(\theta d\ell)_d+\int_0^{\ell_h}(\theta d\ell)_u+\ell_a(\theta_a-\theta_c)\right]-\frac{1}{2\rho_0}\left[\sum_i\frac{f_i\rho_i u_i^2\ell_i}{d_i}+\sum_i K_i\rho_i u_i^2\right]=0.0 \qquad (9)$$

where

$$\ell_a=\frac{L_a}{L_r},\quad d_i=\frac{D_i}{L_r},\quad u_i=\frac{U_i}{U_r}$$

The continuity equation at the i th section of the loop can be written as

$$U_iA_i=A_oU_o$$

where A_0 is a reference flow area and U_o is the velocity at this flow area. The non-dimensional continuity equation is

$$u_i=\frac{A_o}{A_i}u_o$$

and Eq. (9) becomes

$$Ri\left[\ell_a(\theta_a-\theta_c)-\int_0^{\ell_h}(\theta d\ell)_d+\int_0^{\ell_h}(\theta d\ell)_u\right]-\frac{u_o^2}{2}\left[\sum_i\left(\frac{f_i\ell_i}{d_i}+K_i\right)\left(\frac{A_o}{A_i}\right)^2\right]=0.0 \qquad (10)$$

The energy equation for the fluid in the inner pipe is

$$\frac{\pi}{4}D_{Ip}^2U\rho C_p\frac{\partial T_I}{\partial Z}=\pi D_{Ip}h_I(T_{sI}-T_I)$$

or

$$U\rho C_p\frac{\partial T_i}{\partial Z}=\frac{4h_I}{D_{Ip}}(T_{sI}-T_I) \qquad (11)$$

For

$$U=U_ru,\quad Z=L_rz,\quad u=u_o\frac{A_o}{A}$$

the non-dimensional energy equation is

$$u_o \frac{A_o}{A} \frac{\partial \theta_I}{\partial z} = \frac{4 h_I L_r}{\rho C_p U_r D_{Ip}} \left(\theta_{sI} - \theta_I \right)$$

or

$$u_o \frac{A_o}{A} \frac{\partial \theta_I}{\partial z} = St_I \left(\theta_{sI} - \theta_I \right) \tag{12}$$

and

$$St_I = \frac{4 h_I L_r}{\rho C_p U_r D_{Ip}} \tag{13}$$

is the modified Stanton number for the inner tube.

The energy equation for the fluid in the annulus between the RCCS tubes is

$$A_\alpha U \rho C_p \frac{\partial T_e}{\partial Z} = P_e h_{IO} \left(T_e - T_{sI} \right) \tag{14}$$

where h_{IO} is the heat transfer coefficient on the outer surface of the inner tube.

The above equation can be reduced into a non-dimensional equation as

$$u_o \frac{A_o}{A_\alpha} \frac{\partial \theta_e}{\partial z} = St_e \left(\theta_{se} - \theta_e \right) - St_\alpha \left(\theta_e - \theta_{sI} \right) \tag{15}$$

Where St_e and St_α are the modified Stanton numbers for the outer and inner walls of the annulus, respectively, and are given by

$$St_e = \frac{P_e h_\alpha L_r}{\rho C_p U_r A_\alpha} \tag{16}$$

$$St_\alpha = \frac{P_I h_{IO} L_r}{\rho C_p U_r A_\alpha} \tag{17}$$

In a rectangular two-dimensional cavity with one vertical wall heated, the other vertical wall cooled, and the two horizontal walls insulated, the conservation equations for mass, momentum and energy can be written as:

$$\frac{\partial W}{\partial Z}+\frac{\partial V}{\partial Y}=0 \tag{18}$$

$$\rho\left(W\frac{\partial W}{\partial Z}+V\frac{\partial W}{\partial Y}\right)=-\frac{\partial P}{\partial Z}-\bar{\rho}_o g\left[1-\beta\left(T-\bar{T}_o\right)\right]+\mu\left(\frac{\partial^2 W}{\partial Z^2}+\frac{\partial^2 W}{\partial Y^2}\right) \tag{19}$$

$$\rho\left(W\frac{\partial V}{\partial Z}+V\frac{\partial V}{\partial Y}\right)=-\frac{\partial P}{\partial Y}+\mu\left(\frac{\partial^2 V}{\partial Z^2}+\frac{\partial^2 V}{\partial Y^2}\right) \tag{20}$$

$$\rho C_p\left(W\frac{\partial T}{\partial Z}+V\frac{\partial T}{\partial Y}\right)=k\left(\frac{\partial^2 T}{\partial Z^2}+\frac{\partial^2 T}{\partial Y^2}\right) \tag{21}$$

where

P = pressure
W = velocity component in the vertical direction (Z)
V = velocity component in the horizontal direction (Y)
$\bar{\rho}$ = density at the reference temperature $\bar{T}$

and the Boussinesq approximation for the temperature dependence of density has been used in the buoyancy term of Eq. (19).

For

$$z=\frac{Z}{H},\qquad y=\frac{Y}{H} \tag{22a}$$

$$w=\frac{W}{u^*},\qquad v=\frac{V}{u^*},\qquad u^*=\frac{\mu}{\rho H} \tag{22b}$$

$$p=\frac{P+\rho_o g Z}{\rho u^{*2}}\ ,\quad \theta=\frac{T-\bar{T}_0}{T_h-T_c} \tag{22c}$$

Eqs. (18) to (21) become

$$\frac{\partial w}{\partial z}+\frac{\partial v}{\partial y}=0 \tag{23}$$

$$w\frac{\partial w}{\partial z}+v\frac{\partial w}{\partial y}=-\frac{\partial p}{\partial z}+\frac{R\alpha}{\mathrm{Pr}}\theta+\frac{\partial^2 w}{\partial z^2}+\frac{\partial^2 v}{\partial y^2} \tag{24}$$

$$w\frac{\partial v}{\partial z}+v\frac{\partial v}{\partial y}=-\frac{\partial p}{\partial y}+\frac{\partial^2 v}{\partial z^2}+\frac{\partial^2 v}{\partial y^2} \tag{25}$$

$$w\frac{\partial \theta}{\partial z}+v\frac{\partial \theta}{\partial y}=\frac{1}{\mathrm{Pr}}\left(\frac{\partial^2 \theta}{\partial z^2}+\frac{\partial^2 \theta}{\partial y^2}\right) \tag{26}$$

where

$R\alpha = \dfrac{C_p\rho^2 g\beta\left(T_h-T_c\right)H^3}{\mu k}$ = Rayleigh number

$\mathrm{Pr} = \dfrac{C_p\mu}{k}$ = Prandtl number

T_h = temperature of the hot wall

T_c = temperature of the cold wall

$\overline{T}$ = $0.5\ \left(T_h+T_c\right)$

2.2 Transient

In the event that the RCCS has to operate in the natural circulation mode (loss of pumping and loss of water cooling in the RCCS tanks), the system will operate in single phase for a significant length of time. Finally, as the water in the system heats up steam flashing is expected to develop in the upper section of the return lines of the system. In this section, analyses are presented for system operation in single-phase as well as for operation after initiation of flashing.

2.2.1 Operation in Single-Phase Flow

The integrated momentum equation in the i th section, where the flow is incompressible, is

$$\rho\frac{dU_i}{dt}L_i = \Delta p_i - g\int_0^{L_i}\rho dL-\frac{1}{2D_i}f_i\rho_i U_i^2 L_i \tag{27}$$

With the Boussinesq approximation in the gravitational term, the above equation gives

$$\rho\frac{dU_iL_i}{dt} = \Delta p_i - g\rho_o L_i+\rho_0 g\beta\left(T_r-T_o\right)\int_0^{L_i}\theta dL-\frac{1}{2D_i}\rho f_i U_i^2 L_i \tag{28}$$

For a non-dimensional time τ defined as

$$\tau = \frac{U_r t}{L_r} \tag{29}$$

Eq. (28) is written as

$$\rho U_r^2 l_i \frac{du_i}{d\tau} = \Delta p_i - g\rho_0 \ell_i L_r + \rho_0 g\beta \left(T_r - T_o\right) L_r \int_0^{l_i} \theta dL - \frac{1}{2}\frac{\rho}{D_i} f_i U_r^2 u_i^2 L_i$$

and for $\rho \approx \rho_0$

$$l_i \frac{du_i}{d\tau} = \Delta P_i - \frac{gL_r}{U_r^2}\ell_i + Ri\int_0^{\ell_i} \theta dl - \frac{1}{2}\frac{f_i u_i^2 L_i}{D_i} \tag{30}$$

From the non-dimensional continuity equation

$$u_i = \frac{A_0}{A_i} u_0$$

the integral momentum equation in the i th section becomes

$$\ell_i \frac{A_0}{A_i}\frac{du_0}{d\tau} = \Delta P_i - \frac{gL_r}{U_r^2}\ell_i + Ri\int_0^{\ell_i} \theta d\ell - \frac{u_0^2 f_i L_i}{2D_i}\left(\frac{A_0}{A_i}\right)^2 \tag{31}$$

Summation of the above integral momentum equation over all the sections of the loop where the fluid is incompressible (liquid water), and accounting of the other pressure losses (expansions, contractions, bends) gives the overall integral momentum equation as

$$\frac{du_0}{d\tau}\sum_i \ell_i \frac{A_0}{A_i} = R_i \sum_i \int_0^{\ell_i} \theta d\ell - \frac{u_0^2}{2}\sum_i \left(\frac{f_i L_i}{D_i} + K_i\right)\left(\frac{A_0}{A_i}\right)^2 \tag{32}$$

The energy equation for the fluid in the inner pipe is

$$\frac{\pi}{4} D_{Ip}^2 \rho C_p \frac{\partial T_I}{\partial t} + \frac{\pi}{4} D_{Ip}^2 \rho U C_p \frac{\partial T_I}{\partial Z} = \pi D_{Ip} h_I \left(T_{sI} - T_I\right) \tag{33}$$

The non-dimensional form of this equation is

$$\frac{\partial \theta_I}{\partial \tau} + u_o \frac{A_o}{A}\frac{\partial \theta_I}{\partial z} = \frac{4h_I L_r}{\rho C_p U_r D_{Ip}}\left(\theta_{sI} - \theta_I\right)$$

or

$$\frac{\partial \theta_I}{\partial \tau} + u_o \frac{A_o}{A} \frac{\partial \theta_I}{\partial z} = St_I \left(\theta_{sI} - \theta_I \right) \tag{34}$$

The energy equation for the fluid in the annulus between the RCCS tubes is

$$A_\alpha \rho C_p \frac{\partial T_e}{\partial t} + A_\alpha U \rho C_p \frac{\partial T_e}{\partial Z} = P_e h_\alpha \left(T_{se} - T_e \right) - P_I h_{IO} \left(T_e - T_{SI} \right) \tag{35}$$

where h_{IO} is the heat transfer coefficient on the outer surface of the inner tube.

The non-dimensional form of Eq. 35 becomes

$$\frac{\partial \theta_e}{\partial \tau} + u_o \frac{A_o}{A_\alpha} \frac{\partial \theta_e}{\partial z} = St_e \left(\theta_{se} - \theta_e \right) - St_\alpha \left(\theta_e - \theta_{sI} \right) \tag{36}$$

The energy equation for the solid structure in the i th section is

$$\frac{\partial T_s}{\partial t} = \frac{k}{\rho C_p} \frac{\partial^2 T_s}{\partial Z^2} = \alpha_i^* \frac{\partial^2 T_s}{\partial Z^2} \tag{37}$$

For

$$\tau^* = t \frac{\alpha^*}{\delta_i^2} \tag{38}$$

Equation (37) gives

$$\frac{\alpha_i^*}{\delta_i^2} \left(T_r - T_0 \right) \frac{\partial \theta_s}{\partial \tau^*} = \alpha_i^* \frac{T_r - T_0}{L_r^2} \frac{\partial^2 \theta_s}{\partial z^2}$$

or

$$\frac{\partial \theta_s}{\partial \tau^*} = \frac{\delta_i^2}{L_r^2} \frac{\partial^2 \theta}{\partial z^2} \tag{39}$$

For

$$\tau = t \frac{U_r}{L_r}$$

Equation (38) gives

$$\tau^* = \tau \frac{L_r}{U_r} \frac{\alpha_i^*}{\delta_i^2}$$

and Eq. (39) becomes

$$\frac{\partial \theta_s}{\partial \tau} = \left(\frac{\alpha_i^*}{\delta_i^2} \frac{L_r}{U_r} \right) \frac{\delta_i^2}{L_r^2} \frac{\partial^2 \theta_s}{\partial z^2} \tag{40}$$

For the inner and outer pipes of the RCCS, Eq. (40) is written, respectively, as

$$\frac{\partial \theta_{sI}}{\partial \tau} = \left(\frac{\alpha_I^*}{\delta_I^2} \frac{L_r}{U_r} \right) \frac{\delta_I^2}{L_r^2} \frac{\partial^2 \theta_{sI}}{\partial z^2} \tag{41}$$

$$\frac{\partial \theta_{se}}{\partial \tau} = \left(\frac{\alpha_e}{\delta_e^2} \frac{L_r}{U_r} \right) \frac{\delta_e^2}{L_r^2} \frac{\partial^2 \theta_{se}}{\partial z^2} \tag{42}$$

The boundary conditions between the solid and fluid in the pipes of the RCCS are

$$\left. \frac{\partial \theta_{se}}{\partial r} \right|_{r_3} = \frac{h_e \delta_e}{k_{s,e}} \left(\theta_{se} - \theta_e \right) \tag{43}$$

$$\left. \frac{\partial \theta_{sI}}{\partial r} \right|_{r_2} = \frac{h_{IO} \delta_I}{k_{s,I}} \left(\theta_e - \theta_{sI} \right) \tag{44}$$

$$\left. \frac{\partial \theta_{sI}}{\partial r} \right|_{r_1} = \frac{h_I \delta_I}{k_{s,I}} \left(\theta_{sI,I} - \theta_I \right) \tag{45}$$

Where $r = R/\delta$ (non-dimensional radius).

Taking into consideration the radiative heat transfer from the reactor vessel to the outer wall of the outer pipe, the boundary condition at the outer surface of the outer pipe can be written as

$$A_k k_{se} \frac{\partial T_{se}}{\partial R} = A_c h_c \left(T_h - T_{se,o} \right) + A_r \varepsilon \sigma \left(T_h^4 - T_{se,o}^4 \right)$$

or

$$\frac{\partial \theta_{se}}{\partial r} = \frac{A_c h_c \delta_e}{A_k k_{se}} \left(\theta_h - \theta_{se,o} \right) + \frac{\delta_e A_r \varepsilon \sigma T_0^4}{A_k k_{se} \left(T_r - T_o \right)} \left\{ \left[\theta_h \left(\frac{T_r}{T_0} - 1 \right) + 1 \right]^4 - \left[\theta_{se,o} \left(\frac{T_r}{T_0} - 1 \right) + 1 \right]^4 \right\} \quad (46)$$

Where A_k, A_c and A_r are equivalent areas, and $T_{se,o}$ is the temperature of the outer surface of the outer tube.

Before steam flashing is initiated in the RCCS return line, the water in the RCCS tanks is heated up as it mixes with the hot water of the return lines. Taking into consideration that during single-phase operation the tanks do not loose water, the RCCS transient is slow (the system is in a quasi-steady state), and assuming instantaneous mixing, the energy equation for the water in the tanks can be written as

$$A_t H_t \rho C_p \frac{dT}{dt} = A_o \rho U_o \left(t \right) C_p \left(T_{in} - T \right) \quad (47)$$

where T_{in} is the water temperature at the exit of the RCCS heated section. The non-dimensional form of this equation is

$$\frac{d\theta}{d\tau} = \frac{A_o L_r}{A_t H_t} u_o \left(t \right) \left(\theta_{in} - \theta \right) \quad (48)$$

After flashing is initiated, it is assumed that the steam vents to the atmosphere, the system looses water, and the temperature of the water in the tanks remains constant. Then the conservation of mass equation in the tank is of the form

$$\rho A_t \frac{dH_w}{dt} = \rho A_{out} U_{out} \quad (49)$$

For $H_w = h_w H_t$, where H_t is the water height in the tank at steady state conditions, the non-dimensional form of the above equation is

$$\frac{dh_w}{d\tau} = \frac{A_{out} L_r}{A_t H_t} u_{out} \quad (50)$$

2.2.2 Two-phase Flow Section

During a long shutdown transient where decay heat is removed by the RCCS, failure of the tank water cooling system will eventually lead to water boiling and water loss in the RCCS. During this phase of the transient, the description of the system behavior requires the following additional equations.

The acceleration pressure drop due to density change is [5]

$$\Delta p_a = \rho_o^2 U_o^2 \left(\frac{1}{\rho_{m,x}} - \frac{1}{\rho_\ell} \right) \tag{51}$$

where $\rho_{m.x}$ is given by

$$\frac{1}{\rho_{m,x}} = \left[\frac{x_x^2}{\rho_g \alpha_x} + \frac{\left(1 - x_x\right)^2}{\rho_\ell \left(1 - \alpha_x\right)} \right] \tag{52}$$

Substitution of Eq. (52) into Eq. (51) gives

$$\Delta p = \rho_o U_o^2 \left[\frac{x_x^2}{\alpha_x} \frac{\rho_\ell}{\rho_g} + \frac{\left(1 - x_x\right)^2}{\left(1 - \alpha_x\right)} - 1 \right] \tag{53}$$

Other pressure losses (expansions, contractions, bends, exit, etc.), Δp_ℓ, can be computed from [5]

$$\Delta p_\ell = \rho_o U_o^2 K \left(1 + \frac{\Delta \rho}{\rho_g} x^{1.5} \right) \tag{54}$$

The frictional pressure drop Δp_f can be obtained from [5]

$$\Delta p_f = \frac{1}{2} \frac{\rho_o U_o^2}{D} f \left[1 + \frac{x \Delta \rho}{\rho_g} \right] \left[1 + \frac{x \Delta \mu}{\mu_g} \right]^{-0.25} L_b \tag{55}$$

In Eqs. (54) and (55), x can be approximately set equal to $0.50 x_x$.

The gravitational head Δp_g in the vertical boiling section of length L_{vb} is

$$\Delta p_g = g \int_o^{L_{bv}} \rho dL = g \int_o^{L_{bv}} \left[\rho_g \alpha + \rho_\ell \left(1 - \alpha\right) \right] dL = \rho_g L_{bv} - g \Delta \rho \int_o^{L_{bv}} \alpha dL \tag{56}$$

The total non-dimensional pressure drop in the two-phase flow section is

$$\Delta p_{TP} = \frac{u_o^2}{2}\sum_{i,TP}\left\{\frac{f_i \ell_i}{d_i}\left[1+x\frac{\Delta\rho}{\rho_g}\right]_i\left[1+x\frac{\Delta\mu}{\mu_g}\right]_i^{-0.25}\left(\frac{A_o}{A_i}\right)^2 + K_i\left(1+\frac{\Delta\rho}{\rho_g}x^{1.5}\right)_i\left(\frac{A_0}{A_i}\right)^2\right\}$$

$$+\frac{u_o^2}{2}\left[\frac{x_x^2}{\alpha_x}\frac{\rho_\ell}{\rho_g}+\frac{(1-x_x)^2}{(1-\alpha_x)}-1\right]\left(\frac{A_o}{A_b}\right)^2 \tag{57}$$

The non-dimensional gravitational head is

$$\Delta p_{g,TP} = \frac{gL_r}{U_r^2}\ell_{bv} - \frac{gL_r}{U_r^2}\frac{\Delta\rho}{\rho_\ell}\int_o^{\ell_{bv}}\alpha d\ell \tag{58}$$

The non-dimensional quantity

$$F_r = \frac{U_r^2}{gL_r} \tag{59}$$

is the Froude number, and the non-dimensional gravitational head is written as

$$\Delta P_{g,TP} = \frac{1}{F_r}\left[\ell_{bv} - \frac{\Delta\rho}{\rho_\ell}\int_o^{\ell_{bv}}\alpha d\ell\right] \tag{60}$$

After initiation of boiling, the integral momentum equation becomes

$$\frac{du_0}{d\tau}\sum_i \ell_i\frac{A_0}{A_i} = R_i\sum_i\int_0^{\ell_i}\theta d\ell - \frac{u_0^2}{2}\sum_i\left(\frac{f_i\ell_i}{d_i}+K_i\right)\left(\frac{A_0}{A_i}\right)^2$$

$$-\frac{u_o^2}{2}\sum_{i,TP}\left\{\frac{f_i\ell_i}{d_i}\left[1+x\frac{\Delta\rho}{\rho_g}\right]_i\left[1+x\frac{\Delta\mu}{\mu_g}\right]_i^{-0.25}\left(\frac{A_o}{A_i}\right)^2 + K_i\left(1+\frac{\Delta\rho}{\rho_g}x^{1.5}\right)_i\left(\frac{A_0}{A_i}\right)^2\right\}$$

$$-\frac{u_o^2}{2}\left[\frac{x_x^2}{\alpha_x}\frac{\rho_\ell}{\rho_g}+\frac{(1-x_x)^2}{(1-\alpha_x)}-1\right]\left(\frac{A_o}{A_b}\right)^2 - \frac{1}{F_r}\left[\ell_{bv} - \frac{\Delta\rho}{\rho_\ell}\int_o^{\ell_{bv}}\alpha d\ell\right] \tag{61}$$

In the two-phase flow region, conservation of mass can be expressed by the mixture continuity equation

$$\frac{\partial \rho_m}{\partial t} + \frac{\partial}{\partial Z}\left(\rho_m U_m\right) = 0 \tag{62}$$

and the continuity equation for vapor

$$\frac{\partial}{\partial t}\left(\alpha \rho_g\right) + \frac{\partial}{\partial Z}\left(\alpha \rho_g U_m\right) = -\frac{\partial}{\partial z}\left(\frac{\alpha \rho_g \rho}{\rho_m} V_{gj}\right) \tag{63}$$

The mixture (water-vapor) enthalpy (E_m), equation is

$$\frac{\partial}{\partial t}\left(\rho_m E_m\right) + \frac{\partial}{\partial Z}\left(\rho_m U_m E_m\right) = -\frac{\partial}{\partial z}\left[\frac{\alpha \rho_g \rho}{\rho_m} \Delta E_{fg} V_{gj}\right] \tag{64}$$

In the above equations, the assumptions have been made that: (a) the phase change takes place above the heated section and is due to the pressure drop as the fluid approaches the tank, and (b) heat losses in the piping are not significant.

The vapor drift velocity V_{gj} is defined by

$$V_{gj} = U_g - U_j \tag{65}$$

where

$$U_j = \alpha U_g + \left(1-\alpha\right) U_\ell \tag{66}$$

The mixture velocity U_m and the volumetric velocity U_j are related by

$$U_j = U_m + \alpha \Delta \rho V_{gj} / \rho_m \tag{67}$$

where

$$U_m = \left[\alpha \rho_g U_g + \left(1-\alpha\right) \rho_\ell U_\ell\right] / \rho_m \tag{68}$$

and

$$\rho_m = \alpha \rho_g + \left(1-\alpha\right) \rho_\ell \tag{69}$$

It has been shown [7] that for water flashing at atmospheric pressure the GE-Ramp and the Dixon correlations for the drift velocity fit best the experimental predictions. These correlations are [8]:

$$V_{gj} = 2.9\left\{\frac{\left(\rho_\ell - \rho_g\right)\sigma_s g}{\rho_\ell^2}\right\}^{0.25} \qquad \text{Dixon} \qquad (70)$$

$$V_{gj} = R\left\{\frac{\left(\rho_\ell - \rho_g\right)\sigma_s g}{\rho_\ell^2}\right\}^{0.25} \qquad \text{GE-Ramp} \qquad (71)$$

and,

R = 2.9 for $\alpha \le 0.65$

R = 2.9 (1-Δα)/0.35 for α>0.65

The non-dimensional forms of Eqs. (62), (63) and (64) are

$$\frac{\partial \rho_m^*}{d\tau} + \frac{\partial}{\partial z}\left(\rho_m^* u_m\right) = 0 \qquad (72)$$

$$\frac{\partial}{\partial \tau}\left(a\rho_g^*\right) + \frac{\partial}{\partial z}\left(\alpha\rho_g^* u_m\right) = -\frac{\partial}{\partial z}\left[\alpha\frac{\rho_g^*\rho_\ell^*}{\rho_m^*}V_{gj}^*\right] \qquad (73)$$

$$\frac{\partial}{\partial \tau}\left(\rho_m^* E_m^*\right) + \frac{\partial}{\partial z}\left(\rho_m^* u_m E_m^*\right) = -\frac{\partial}{\partial z}\left(\frac{\alpha\rho_g^*\rho_\ell^*}{\rho_m^*}\Delta E_{fg}^* V_{gj}^*\right) \qquad (74)$$

3.0 Similarity Relations

In this section, the non dimensional groups derived in the previous sections are used to determine approximate similarity relations between the prototype and its simulation at NSTF.

3.1 Single Phase

The heat, $Q(t)$, transferred from the reactor vessel to the RCCS at time t can be roughly approximated by

$$Q(t) = A_c h_{cav}\left(T_h - T_{se,o}\right) + A_{rad}\varepsilon\sigma\left(T_h^4 - T_{se,o}^4\right) \qquad (75)$$

where: A_c and A_{rad} are equivalent areas of heat transfer by convection and radiation; h_{cav} is the heat transfer coefficient for heat transfer in the reactor cavity by convection; and T_h is an average temperature of the reactor vessel. At steady state

$$Q(o) = A_o U_o \rho_o C_p \left(T_r - T_o\right)$$

where T_r and T_o are the inlet and outlet temperatures at the heated section of the RCCS. Equation (75) can be non-dimensionalized as

$$\frac{Q(o) f(t)}{U_o A_o \rho_o C_p \left(T_r - T_o\right)} = f(t) = \frac{A_c h_{cav}}{A_o \rho_o C_p U_o}\left(\theta_h - \theta_{se,o}\right) + \frac{A_{rad} \varepsilon \sigma T_o^4}{U_o A_o \rho_o C_p \left(T_r - T_o\right)}$$

$$\left\{\left[\theta_h\left(\frac{T_r}{T_o} - 1\right) + 1\right]^4 - \left[\theta_{se,o}\left(\frac{T_r}{T_o} - 1\right) + 1\right]^4\right\} \tag{76}$$

where $Q(t)$ has been written as

$$Q(t) = Q(o) f(t) \tag{77}$$

Equation (76) introduces the non-dimensional groups

$$\frac{A_c h_{cav}}{A_o \rho C_p U_o},\ \frac{A_{rad} \varepsilon \sigma T_o^4}{U_o A_o \rho_o C_p \left(T_r - T_o\right)},\ \text{and}\ \frac{T_r - T_o}{T_o} \tag{78}$$

which are here denoted as the "cavity convective number", *Nc*, the "cavity radiation" number, *Nr*, and the "temperature ratio" number, *Nt*, respectively.

For the scaled NSTF model of the RCCS to be similar to the prototype RCCS, the ratio of the value of a similarity group at NSTF conditions to the value of the same group at prototype conditions must be equal to one. In the analysis that follows, the subscript R denotes the ratio of the value of a parameter in the model to the value of the same parameter in the prototype. Thus

$$\psi_R = \frac{\psi(model)}{\psi(prototype)} = \frac{\psi_m}{\psi_p} \tag{79}$$

At NSTF the same materials will be used as in the prototype. Therefore, $\psi_R = 1.0$ for any material property ψ (strictly at the same temperature).

After the geometric similarity condition is decided, the similarity condition for the friction number

$$\left[\sum_i F_i \left(\frac{A_o}{A_i}\right)^2\right]_R = \left[\sum_i \left(\frac{f_i L_i}{D_i} + K_i\right)\left(\frac{A_o}{A_i}\right)^2\right]_R = 1.0 \tag{80}$$

can be easily satisfied by using appropriate orifices.

Taking the heated section as the reference section, at steady state conditions, the temperature rise, ΔT_o, along the heated section is

$$\Delta T_o = \frac{\dot{Q}}{U_o A_o \rho_o C_p} = T_r - T_o \tag{81}$$

Where T_r and T_o are the temperatures at the inlet and exit of the heated section. From the above definition of the reference section

$$L_r = L_h \ , \ U_r = U_o$$

Insertion of the above expression for ΔT_o into the steady state integral momentum equation gives

$$U_o = \left\{ \frac{g\beta\dot{Q}}{A_o \rho_o C_\rho} \left[\frac{L_c + \frac{1}{2} L_h}{\frac{1}{2}\sum_i \frac{f_i L_i}{D_i}\left(\frac{A_o}{A_i}\right)^2 + \frac{1}{2}\sum_i K_i \left(\frac{A_o}{A_i}\right)^2} \right] \right\}^{1/3} \tag{82}$$

If

$$\left[\sum_i F_i \left(\frac{A_O}{A_i} \right)^2 \right]_R = 1.0$$

then

$$U_{OR} = \left\{ \frac{\dot{Q}_R}{A_{OR}} \left(L_c + \tfrac{1}{2} L_h \right)_R \right\}^{1/3} \tag{83}$$

From Eq. (81)

$$\Delta T_{oR} = \frac{\dot{Q}_R}{U_{oR} A_{oR}} \tag{84}$$

and the Richardson number ratio becomes

$$Ri_R = \frac{\dot{Q}_R L_{hR}}{U_{oR}^3 A_{oR}} \tag{85}$$

Use of Eq. (83) gives

$$Ri_R = \frac{L_{hR}}{\left(L_c + \frac{1}{2} L_h\right)_R} \tag{86}$$

From the geometric similarity (same in all directions)

$$\ell_R = L_{hR} = L_{cR}$$

and the similarity condition from the Richardson number gives

$$Ri_R = \frac{\ell_R}{\ell_R} = 1$$

Thus, with the U_o and ΔT_o scaling given by Eqs. (83) and (84) the similarity requirement $Ri_R = 1$ is automatically satisfied.

The time number, T^*, similarity requires

$$T_R^* = \frac{L_{hR}}{U_{oR} \delta_{i\,R}^2} = 1$$

For $\delta_{iR} = \ell_R$, the above equation gives

$$U_{oR} \ell_R = 1, \text{ or } U_{oR} = \frac{1}{\ell_R} \tag{87}$$

Then, from the Richardson number

$$\frac{\Delta T_{oR} \ell_R}{U_{oR}^2} = 1$$

and

$$\Delta T_{oR} = \frac{U_{oR}^2}{\ell_R} = \frac{1}{\ell_R^3} \tag{88}$$

$$\Delta T_{o,m} = \frac{\Delta T_{o,p}}{\ell_R^3}$$

If $\ell_R = 0.5$, then

$$\Delta T_{oR} = 8, \text{ and } \Delta T_{o,m} = 8\Delta T_{o,p}$$

Similarly, from Eq. (81) and from $A_{oR} = \ell_R^2$

$$\dot{Q}_R = \frac{1}{\ell_R^2} = 4$$

and

$$\dot{Q}_m = 4Q_p$$

The power $\dot{Q}$ transferred from the reactor vessel to the RCCS is

$$\dot{Q} = q^{"}\delta_y L_{Rv} \tag{89}$$

where δ_y is the width of the RCCS cell (section) simulated at NSTF and L_{Rv} is the height of the reactor vessel.

Then,

$$\dot{Q}_R = q_R^{"}\delta y_R \ell_R = q_R^{"}\ell_R^2$$

And from Eq. (89)

$$q_R^{"} = \frac{1}{\ell_R^4} \tag{90}$$

For $\ell_R = 1/2$

$$q_m^{"} = 16 q_p^{"} \tag{91}$$

Equation (91) imposes an excessive requirement on the model (NSTF) heat flux. To overcome this difficulty, the similarity requirements need to be relaxed.

If $\delta_{iR} = 1$ (similarity requirement for thickness is relaxed), the time ratio T_R^* becomes

$$T_R^* = \frac{L_{hR}}{U_{oR}}$$

For a real time simulation $T_R^* = 1$, and

$$U_{oR} = L_{hR} = \ell_R \tag{92}$$

Then, from $Ri_R = 1$,

$$\frac{\Delta T_{oR} \ell_R}{U_{oR}^2} = \frac{\Delta T_{oR} \ell_R}{\ell_R^2} = \frac{\Delta T_{oR}}{\ell_R} = 1$$

or

$$\Delta T_{oR} = L_{hR} = \ell_R \tag{93}$$

and from the steady state energy balance Eq. (81)

$$\dot{Q}_R = \ell_R^2 A_{oR}$$

The power $\dot{Q}$ transferred from the reactor vessel to the RCCS is

$$\dot{Q} = q'' \delta y L_{Rv}$$

and

$$\ell_R^2 A_{oR} = q_R'' \delta y_R \ell_R$$

For $D_R = \delta y_R$

$$q_R'' = \ell_R D_R \tag{94}$$

The similarity requirement imposed by the Stanton number is

$$St_R = \frac{h_R \ell_R}{U_{oR} D_R} = 1.0$$

where h_R is the ratio o f the heat transfer coefficient.

For $U_{oR} = \ell_R$ (Eq. (92))

$$St_R = \frac{h_R}{D_R} = 1.0$$

or

$$h_R = D_R$$

If the flow is turbulent and the heat transfer coefficient is given by a relation of the form (Dittus-Boelter correlation)

$$Nu = 0.023\,\mathrm{Re}^{0.8}\,\mathrm{Pr}^{0.4} = \frac{hD}{k}$$

Then

$$h_R = \frac{\left(U_{oR} D_R\right)^{0.8}}{D_R} = \ell_R^{0.8} D_R^{-0.2}$$

For $h_R = D_R$, the above relation gives

$$D_R^{1.2} = \ell_R^{0.8} \tag{95}$$

For $\ell_R = 0.5$, the above relation gives $D_R = 0.630$, or $D_R \approx \ell_R$. For $D_R = \ell_R$,

$$\mathrm{Re}_R = U_R D_R = \ell_R^2$$

and for $\ell_R = 0.5$, the Re ratio becomes $\mathrm{Re}_R = 0.25$. This means that it needs to be assured that the flow in the scaled model remains turbulent.

The cavity radiation number, Nr, gives

$$Nr_R = \frac{\ell_R \delta y_R T_{oR}^4}{\ell_R D_R^2 \ell_R} = \frac{T_{oR}^4}{D_R \ell_R} = 1$$

For $D_R = \ell_R = 1/2$

$$T_{oR}^4 = \ell_R^2$$

or

$$T_{oR} = \sqrt{\ell_R} = 0.707$$

From

$$\Delta T_{oR} = T_{oR}\left(\frac{T_r}{T_o} - 1\right)_R = \ell_R$$

The temperature ratio number gives

$$Nt_R = 0.707$$

versus $Nt_R = 1$ that the similarity condition requires.

The cavity convective number, Nc, gives

$$Nc_R = \frac{\ell_R \delta y_R h_{cavR}}{D_R^2 \ell_R} = \frac{h_{cavR}}{D_R}$$

or

$$h_{cavR} = Nc_R D_R = D_R$$

If the heat transfer coefficient in the cavity is given from (Ref. 4)

$$Nu = 0.046 R\alpha^{1/3}$$

then

$$h_{cavR}\ell_R = \left[\left(T_h - T_c\right)_R \ell_R^3\right]^{1/3}$$

and

$$h_{cavR} = \left(T_h - T_c\right)_R^{1/3}$$

Some analysis is needed to evaluate how close the above value is to

$$h_{cavR} = Nc_R D_R = D_R$$

If scaling in the lateral direction is modified and D_R is set equal to one, i.e.,

$$D_R = \delta_{iR} = \delta_{yR} = 1.0$$

then the process described above gives

$$q''_R = \ell_R$$
$$St_R = h_R = 1.0$$

but $h_R = \ell_R^{0.8}$ from the heat transfer correlation (Dittus-Boelter), and for $\ell_R = 0.5$: $h_R = 0.57$, and $\mathrm{Re}_R = 0.5$. From $Nc_R = 1$, we get $T_{oR} = \ell_R^{1/4}$, and $Nt_R = \ell_R^{3/4}$, or $T_{oR} = 0.84$, and $Nt_R = 0.59$ (for $\ell_R = 0.5$). The similarity condition for the cavity

convective number requires $Nc_R = h_{cavR} = 1.0$, but the heat transfer correlation in the cavity gives

$$h_{cavR} = \left(T_h - T_c\right)_R^{1/3}$$

The similarity conditions imposed by the boundary conditions between the solid and the fluid in the pipes requires

$$Bi_R = h_R \delta_{iR} = 1.0$$

or $h_R = 1.0$ for $\delta_{iR} = 1.0$. This is the same condition imposed by $St_R = 1.0$ for $\delta_{iR} = D_R = 1.0$.

The similarity conditions for the mass and energy equations in the tank require

$$\left(\frac{A_{out} L_r}{A_t H_t}\right)_R = 1, \qquad \left(\frac{A_o L_r}{A_t H_t}\right)_R = 1$$

which are geometric similarity condition and are automatically satisfied.

From the above analysis it is clear that all similarity conditions cannot be satisfied. At this time no specific information is available on the prototype water-cooled RCCS. When this information becomes available, some analyses with the prototype and the model will provide information on the magnitude of distortions imposed by the similarity conditions that are not satisfied.

3.2 Two-Phase Flow

At this time no detailed design information and no analysis is available for a reference water-cooled RCCS design. For the purposes of this work, it is assumed that: (a) during the transient time that credit is taken for passive heat removal by the RCCS, boiling in the stand-pipes is not significant, and (b) the two-phase flow in the pipes above the RCCS heated section is due to flashing.

In the two-phase flow section, the non-dimensional groups are [9]:

Froude number: $$N_{Fr} = \left(\frac{U_0^2}{g L_r}\right)\frac{\rho_f}{\Delta\rho} \tag{96}$$

Friction number: $$N_{fi} = \left(\frac{fl}{d}\right)_i \left[\frac{1 + x\left(\Delta\rho/\rho_g\right)}{\left(1 + x\,\Delta\mu/\mu_g\right)^{0.25}}\right]\left(\frac{A_o}{A_i}\right)^2 \tag{97}$$

Orifice number: $$N_o = K_i \left[1 + x^{3/2}\left(\Delta\rho/\rho_g\right)\right]\left(\frac{A_o}{A_i}\right)^2 \quad (98)$$

Drift flux number: $$N_d = \frac{V_{gj}}{U_o} \quad (99)$$

Similarity requires $\left(N_{Fr}\right)_R = \left(N_{fi}\right)_R = \left(N_{oi}\right)_R = \left(N_d\right)_R = 1.0$. The similarity condition for the Froude number requires

$$U_{oR} = \sqrt{\ell_R} \quad (100)$$

For $\delta_{iR} = 1$ and $U_{oR} = \sqrt{\ell_R}$, the similarity condition for the time number gives

$$T_R^* = \frac{\ell_R}{U_{oR}} = \sqrt{\ell_R} \quad (101)$$

The above equation indicates that in a reduced-height model the time-scale of the events is shortened.

Using the Dixon correlation Eq. (70) for V_{gj}, the ratio of the drift flux number becomes

$$\left(N_d\right)_R \approx \frac{1}{U_{oR}} = \frac{1}{\sqrt{\ell_R}} \quad (102)$$

For $\ell_R = 0.5$, Eq (102) gives

$$\left(N_d\right)_R \approx 1.4$$

The friction and orifice numbers Eqs. (97) and (98) are functions of the same quantities for single-phase RCCS flow, of the void fraction, and of properties of saturated liquid and steam. Their similarity ratios can be approximated by their single-phase values.

The RCCS pipes vent steam into the water tanks, and from there the steam is vented to the atmosphere. Depending on the design of this venting system, some water from the tanks may be carried out with the steam. Because no design information is available for the venting system, its scaling will not be considered here.

For $U_{oR} = \sqrt{\ell_R}$ and from $Ri_R = 1.0$, we get $\Delta T_{oR} = 1$

Then, Eq. (81) gives

$$\Delta T_{oR} = \frac{\dot{Q}_R}{U_{oR} A_{oR}} = 1$$

and for $A_{oR} = 1.0$

$$\dot{Q}_R = U_{oR} = \sqrt{\ell}_R$$

From Eq. (89)

$$q''_R = \frac{\dot{Q}_R}{\delta_{yR} \ell_R}$$

and for $\delta_{yR} = 1.0$,

$$q''_R = \frac{1}{\sqrt{\ell_R}}$$

Table 2 gives the different scaling ratios as a function of the height scaling ratio ℓ_R and their numerical values for $\ell_R = 0.5$. The scaling ratio T_{oR} and the geometric scaling ratios in the lateral direction (D_R, A_{oR}, δ_{iR}, δ_{yR}) have been set equal to one.

Table 2. Scaling Ratios

Scaling Ratios	**Values for** $\ell_R = 0.5$
$(N_{Fr})_R = 1$	1
$\delta_{iR} = 1$	1
$V_{oR} = \sqrt{\ell_R}$	0.707
$T_R^* = \sqrt{\ell_R}$	0.707
$(Ri)_R = 1$	1
$\Delta T_{oR} = 1$	1
$T_{oR} = 1$	1
$D_R = \delta_{yR} = 1$	1
$A_{oR} = 1$	1
$q''_R = \ell_R^{-0.5}$	1.414
$(Nd)_R = \ell_R^{-0.5}$	1.414
$(\mathrm{Re})_R = \sqrt{\ell_R}$	0.707
$h_R = \ell_R^{0.4}$	0.758
$St_R = \ell_R^{0.9}$	0.536
$(Nr)_R = \sqrt{\ell_R}$	0.707
$(Nt)_R = 1$	1
$(Bi)_R = h_R = \ell_R^{0.4}$	0.758

4.0 Simulation of Heat Transfer in Cavities

In the RCCS, heat is transferred from the reactor vessel to the RCCS tubes by radiation and natural convection. Depending on the arrangement of the tubes inside the cavity, the heat transferred by convection can be a significant fraction of the total heat transfer. From available generic information on the water-cooled RCCS system of PBMR, it seems that in such a system convection is very significant.

There is a significant body of experimental work in the literature on natural convection in cavities. In CFD codes, the heat transfer from walls to a fluid is computed directly using the molecular conductivity of the fluid and the turbulent conductivity computed from the turbulent viscosity predicted by a turbulence model, typically a RANS (Reynolds Averaged Navier Stokes) model.

By necessity, the scaling presented in this report is based on a number of approximations, and because no analytical information is available on the performance of a reference water-cooled RCCS, the scaling analysis presented here needs to be "validated" by analysis of the steady state and transient performance of a reference water-cooled RCCS design. This analysis will be based on RCCS simulations with CFD and system codes and the use of available experimental data. The work presented in this section is a first step towards such a "validation". More specifically, its objective is to initiate an assessment of the ability of RANS models to predict with adequate accuracy the heat transfer by natural convection in cavity geometries that are of interest in reactor cavity cooling systems, and in cavity configurations where natural convection is a significant mode of heat transfer.

In RCCS systems, the aspect ratio of the cavity (H/W= height/width) is large, greater than ten, and the Rayleigh (Ra) number is also large. In this work, the experiments of MacGregor and Emery [10] have been analyzed. In these experiments measurements of net heat transfer were performed in a rectangular cavity for Pr numbers of 1 to 20,000, aspect ratios H/W = 10, 20, and 40, and Ra values of: $10^4 < Ra < 10^{12}$. The measurements were performed using as fluid: glycerin, castor oil, water and ethyl alcohol. For large Ra numbers, where the flow is turbulent, MacGregor and Emery derived from their experimental measurements the correlation

$$Nu = 0.046Ra^{1/3}, \qquad 10^6 < Ra$$

In the CFD simulations, water was used as the fluid. For the results presented here an aspect ratio of 10 was used, and the Ra number was varied from 10^{11} to 10^{12} (the upper range of the experimental data). Computations were performed considering the flow as laminar as well as turbulent. The same computational grid was used for the laminar and the turbulent simulations. The grid was fine enough to resolve the boundary layer (200,000 computational cells). For the simulation of turbulence a number of models were used that resolve the boundary layer (no approximation with the law of the wall). These include the standard low Re number k-ε model [11], Suga's low Re number k-ε model [12], and the V2F model [13].

In the low-Re number model, the turbulent viscosity is computed from

$$\mu_t = f\frac{C_\mu \rho k^2}{\varepsilon} \tag{103}$$

where C_μ is a constant, ρ is the fluid density, k is the kinetic energy of turbulence, ε is its rate of dissipation and f is a damping function. In the standard low-Re number model, this function is given by

$$f = \left[1 - e^{-0.0198\,\mathrm{Re}_y}\right]\left(1 + \frac{5.29}{\mathrm{Re}_y}\right) \tag{104}$$

where

$$\mathrm{Re}_y = \frac{y\sqrt{k}}{\nu}$$

y is the normal distance to the wall, and ν is the kinematic viscosity. Suga's low-Re number model also uses an exponential damping function but of a different form than Eq. (104).

In Reference 4, the experimental measurements are presented as a plot of the logarithm of the Nusselt number versus the logarithm of the Rayleigh number. As shown in Table 3, (a) the predictions of the standard and Suga's low-Re models are very close to those obtained by treating the flow as laminar, and (b) although the discrepancy between the predicted and experimental logarithmic value of the Nusselt number is not large, the discrepancy between measured and predicted heat transfer is large. The predictions of the V2F model are also significantly off. An analysis of the velocity and turbulent viscosity distributions predicted by the RANS models shows that in the near-wall layer where the velocity values are of significant magnitude, the turbulent viscosity, and subsequently the turbulent conductivity, are nearly equal to zero. This indicates that the damping function f over-dampens the turbulence in the near-wall layer that is of significance for convection (velocities of significant magnitude).

Table 3. CFD Predictions of Heat Transfer
(constant wall temperature)

Log10Nu: Experiment/CFD					
Ra/Model	Laminar	Standard	Standard Modified	Suga's	V2F
0.84 e11					0.967
1.27 e11	1.028	0.998	1.005		
1.00 e12	1.049	1.048	1.002	1.053	
Heat Transferred: Experiment/CFD					
0.84 e11					0.833
1.27 e11	1.160	0.992	1.0026		
1.00 e12	1.330	1.323	1.011	1.359	

To reduce damping of turbulence in the near-wall region, a modified damping function was defined as

$$f_m = 0.4 + 0.6f \tag{105}$$

As Table 1 shows, this modified function gives predictions that are in a very good agreement with the experimental measurements. Analyses of the predicted kinetic energy of turbulence and of the turbulent viscosity also confirm a reduced damping of turbulence in the near-wall region. The results of this work are also in agreement with the results of Ref. 9, which showed that the standard low-Re number model predicts correctly the shape of the heat transfer coefficient in a buoyant flow in a vertical tube, but under-predicts its magnitude. The validity of the actual form (which may be different than that of Eq. (105) of the modified damping function for buoyant flows needs to be extensively tested with additional experimental data, including that used in [14].

In conclusion, this work shows that for the natural convection flows analyzed here: (a) the heat transfer predictions of the RANS models are significantly off, (b) the damping function used in the low-Re number models over-dampens the turbulence in the near-wall region, and (c) for the flows analyzed here, a modified damping function used with the low-Re number model drastically improves the predictions.

5.0 Scaling Recommendations

A scaling analysis of a water-cooled RCCS system was performed based on generic information on the RCCS design of PBMR. The analysis demonstrates that the water-cooled RCCS can be simulated at the ANL NSTF facility at a prototypic scale in the lateral direction and about half scale in the vertical direction. Because, by necessity, the scaling is based on a number of approximations, and because no analytical information is available on the performance of a reference water-cooled RCCS, the scaling analysis presented here needs to be "validated" by analysis of the steady state and transient performance of a reference water-cooled RCCS design. The analysis of the RCCS performance by CFD and system codes presents a number of challenges including: strong 3-D effects in the cavity and the RCCS tubes; simulation of turbulence in flows characterized by natural circulation, high Rayleigh numbers and low Reynolds numbers; validity of heat transfer correlations for system codes for heat transfer in the cavity and the annulus of the RCCS tubes; the potential of nucleate boiling in the tubes; water flashing in the upper section of the RCCS return line (during limiting transient); and two-phase flow phenomena in the water tanks. The limited simulation of heat transfer in cavities presented in Section 4.0 strongly underscores the need of experimental work to validate CFD codes, and heat transfer correlations for system codes, and to support the analysis and design of the RCCS.

6.0 RCCS Scaled Experimental Simulation

The previous sections have provided the technical basis for properly scaled tests within NSTF to provide water-based RCCS performance data for code verification and

validation under both normal and off-normal (i.e., passive) operating conditions. The purpose of this section is to provide a high-level description of the experiment approach for meeting these data needs. To that end, the technical requirements for the facility are described first. This is followed by a summary description of the overall mechanical, instrumentation, and operational approaches for satisfying these requirements. A more detailed facility/test plan for the water-based RCCS test facility is provided in [14].

6.1 Requirements for Water-Based RCCS Test Facility

As noted previously, although a specific design has not yet been selected for the VHTR, the PBMR water-based RCCS is used as a planning basis for the purposes of this study since that design is mature enough that an appropriately scaled experiment can be developed. Approximate characteristics of this system are summarized in Table 4, while generic system features were shown previously in Fig. 4. The prototype consists of a series of oval standpipes surrounding the reactor vessel to provide cooling of the reactor cavity during both normal and off-normal operating conditions. The standpipes are headered in groups of four to water supply tanks that are situated well above the reactor vessel to facilitate natural convection cooling during loss of forced flow sequences. During normal operations, the water is pumped through a closed circuit that includes the standpipes that extract heat from the reactor cavity, and dump the heat in a sink that is located outside the containment. The oval standpipes are roughly 25 cm x 50 cm, and are in the range of 20 m high. The overall height of the system (which is distance form the bottom of the standpipes to the top of the header tanks) is ~ 40 m.

During off-normal (passive) system operations, forced convection water cooling in the RCCS is lost. In this case, water is passively drawn from an open line located at the bottom of each header tank. Again, the particulars are design-dependent, but for the PBMR system this line is orificed so that flow bypass during normal operations is small, yet the line is large enough to provide adequate flow during passive operations to remove decay heat while maintaining acceptable fuel temperatures. In the passive operating mode, water flows by natural convection from the supply tank to the standpipes, and returns through the normal pathway to the top of the tanks. After the water reaches saturation and boiling commences, steam will pass through the top of the tanks and vent to the atmosphere.

The system described above defines the key physical elements to be included within the test facility so that system behavior during both normal and passive operational modes can be reasonably simulated. As described later in this section, NSTF can accommodate up to three water standpipes with full scale cross-section. For systems that rely on natural convection, similitude between the experiment and prototype can rarely be achieved unless the scale of the experiment is selected to match the prototype. On this basis, the cross-sectional scale of the experiment is selected to be nominally 1:1 with respect to the PBMR system. Given the overall available height within the NSTF high bay of ~ 16 m, then the vertical scaling of the facility is selected be ~ ½. As deduced as part of the scaling analysis, a system that is full scale in cross section and ½ scale vertically can best achieve similitude with the prototype if the heat flux delivered to the standpipes is ~ 40 %

in excess of the prototype. Thus, this is the approach that is adopted for the NSTF water-based RCCS experiment design; namely, fabricate a full-scale cross-section, ½ scale vertical facility that reasonably replicates the overall physical structure of the prototype (PBMR) RCCS. Overall system characteristics are summarized in Table 4.

Table 4. Characteristics of Prototype Water-Based RCCS and Scaled Experiment

Parameter	**Prototype**	**NSTF Scaled Model**
Total number of water standpipes	~ 70	3
Number of tubes per header tank	~ 4	3
Standpipe cross sectional area	~ 25 x 50 cm	Same
Standpipe Length	~20 m	8.1 m
Total elevation difference between header tank and standpipes	~ 40 m	16.1 m
Facility scale	N/A	1:1 radially, ~½ vertically
Vessel wall peak heat flux during normal/off normal conditions	3 - 5 kW/m^2	1.4•prototype for similitude (heater capability: 21 kW/m^2)
Vessel wall peak temperature	~350 ˚C	Same (heater capability:1200˚C)
Standpipe boil-down time at peak heat flux without makeup water	~70 hours	Properly scaled

Based on the above discussion as well as the supporting analyses that have been conducted as part of this work, high level experiment design requirements for the NSTF were established. These requirements are summarized in Table 5. The first requirement is to mock up the actual geometry of the RCCS to the greatest extent possible given the physical constraints of the facility. The approach by which this issue is addressed has just been described. The remaining four requirements are data-related. Namely, measurements of the axial and radial temperature and heat flux distributions on the standpipe walls are required. In addition, data on the standpipe interior water temperature distributions are needed. This collection of measurements will provide the necessary data to evaluate heat transfer coefficients not only axially along the standpipe length, but also radially around the extent of the pipe walls. Finally, void fraction measurements are needed in the return piping from the standpipes to the header tank in order to characterize performance during passive system operations for system-level code validation purposes.

This information forms the basis for the facility modification plan that is provided in the next section.

Table 5. Requirements and Approach for Satisfying Water-Based RCCS Data Needs

	Requirement	Approach	Notes
1	Mock-up water RCCS geometry under prototypic flow conditions	Three (3) 8.1 m long standpipes with prototypic cross-section installed in heated section of NSTF. Peripheral area around tubes sealed at top and bottom to achieve prototypic flow geometry. Apply prototypic surface temperature and/or heat flux boundary conditions to achieve prototypic flow patterns.	Tube dimensions based on an existing design, but other designs can be accommodated.
2	Obtain data on the water, standpipe, and cavity axial temperature distributions under prototypic flow conditions.	Highly instrument the center standpipe cavity walls to measure cavity surface and standpipe internal and external surfaces temperatures at 6 axial positions along the heated length. Obtain measurements on both the heated and unheated cavity walls and the standpipes.	1. Key information for CFD code V&V under prototypic VHTR air RCCS flow conditions. 2. Data from 2-4 provides information needed to evaluate heat transfer coefficients vs. axial position within the standpipes.
3	Obtain data on the standpipe heat flux distributions at prototypic RCCS flow conditions.	Instrument both radially and axially the center standpipe with heat flux meters to provide direct measurements of the heat flux distributions around the pipe at 6 axial elevations.	
4	Obtain data on the cavity bulk gas velocity and temperature distributions.	Utilize insertable hot wire anemometers (back-up: pitot tubes) with co-located, radiation-shielded, thermocouples to measure bulk gas velocity and gas temperature distributions at ~ 1 meter axial increments.	
5	Obtain data on voiding in the return piping from the standpipes to the header tanks	Instrument pipe sections with differential pressure transducers to determine the void fraction as a function of position.	

6.2 Summary of Modifications to Mock Up Water RCCS

As noted above, the approach for mocking up the water RCCS geometry is to try to match the prototype geometry to the greatest extent possible given the facility size constraints. This is accomplished by installing three water standpipes of prototypic cross-section, wall thickness, and pitch in the heated section of NSTF. The standpipe fabrication details are shown in Fig. 5, while the pipe mounting and headering approaches are illustrated in plan view in Figs. 6 and 7. The overall tube length is 8.1 m, which provides sufficient length to mechanically attach the standpipes at the top of the heated portion of the facility, pass through the entire 6.7 m long heated test section length, and penetrate through the bottom of the base support weldment with sufficient clearance to mechanically support the pipes and provide feed throughs for internal instrumentation. As shown in Fig. 7, the top flange of the upper heated section will be modified to receive a support stand for the three standpipes. In addition, the test section support framework will be modified to allow the heated cavity width to be incrementally increased from the current width of 30 cm up to 103 cm. This approach will allow flexibility to accommodate different RCCS air- or water-based designs should the need arise. Furthermore, this would also provide for the possibility to conduct large, open cavity natural convection experiments at Rayleigh numbers that have not been addressed in the literature.

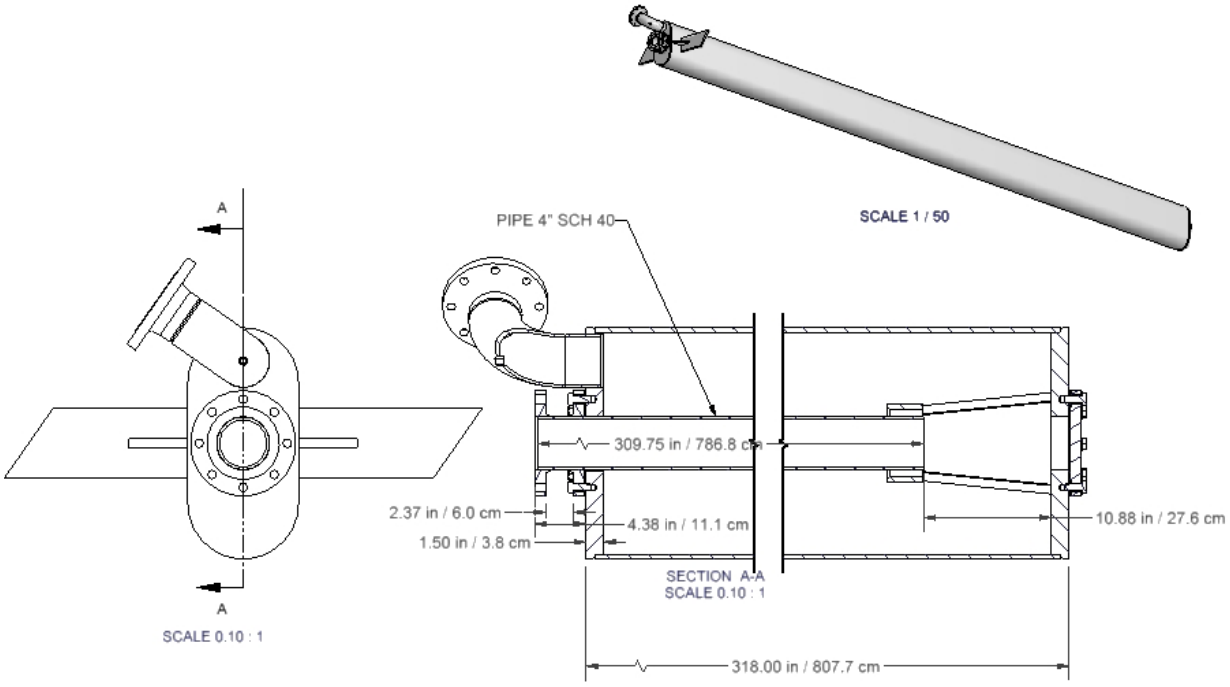

Fig. 5. Details of Water Standpipe Design

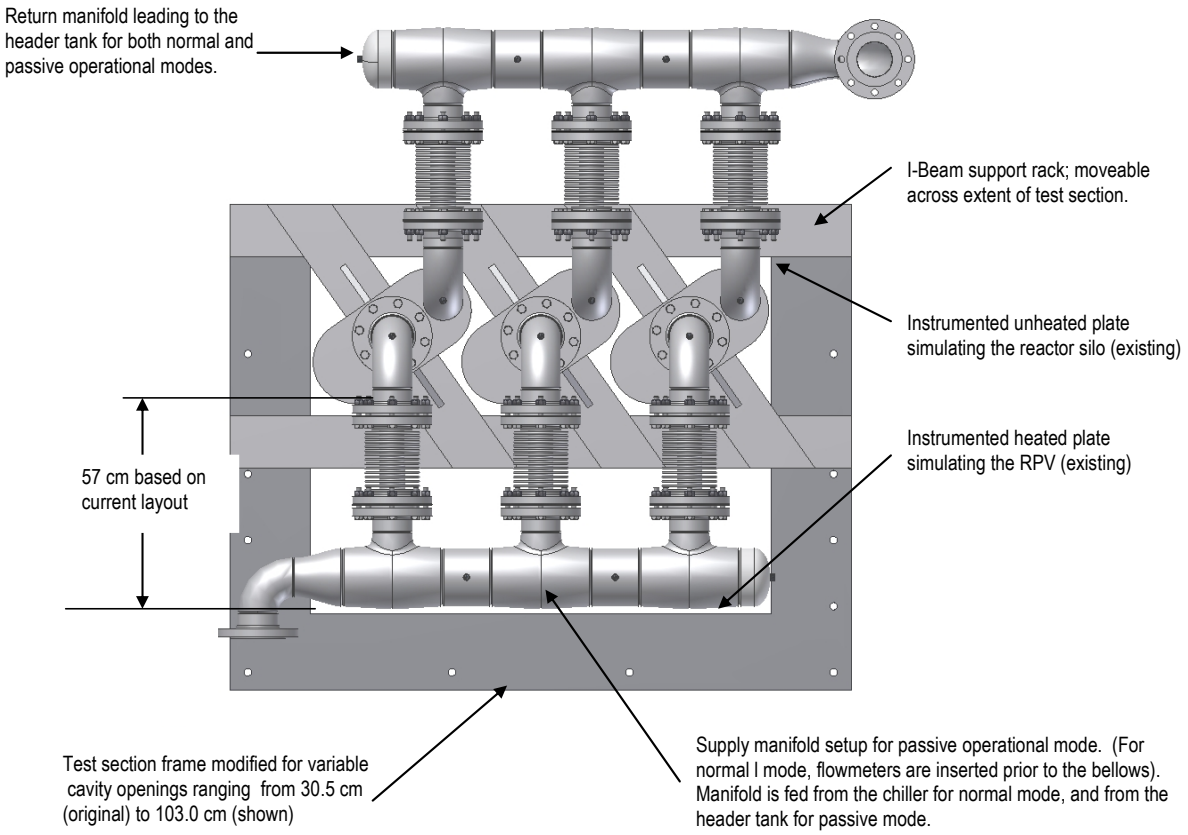

Fig. 6. Key Design Features and Headering Approach for Standpipes

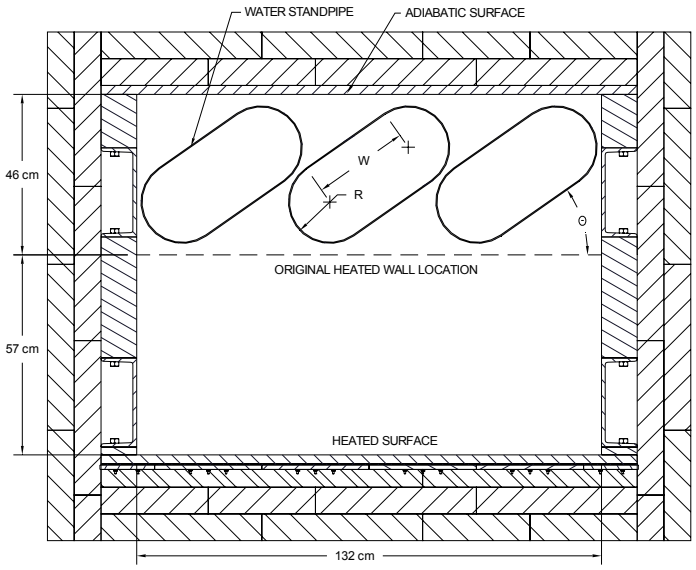

Fig. 7. Cross Section of Test Assembly Showing Principal Details

The standpipes will be suspended (hung) from the test section support plate. The support plate also seals off the available space exterior to the standpipes, thereby providing a stagnant air environment that is consistent with the PBMR design. An alignment plate will be used to ensure proper positioning of the standpipes within the opening at the lower heated section inlet. The alignment plate also seals off the bottom of the section to produce the proper boundary condition for the RCCS piping enclosure. The alignment plate will not be rigidly attached to the pipes, so that tube thermal expansion can be accommodated (< 2 cm) during the tests.

The 6.7 m long heated length of the test section is broken down into 10 equally spaced zones. The power control system will consist of 10 independent control units, one for each of the axial heating zone segments. Each zone can be operated in either temperature or heat flux control modes, so that a wide variety of boundary conditions can be applied during the tests.

In terms of instrumentation, the approach for satisfying key RCCS data needs is summarized in Table 5. As is evident from the table, one of the most important requirements is to obtain data on the standpipe and cavity wall axial and radial temperature distributions under prototypic flow conditions. Both the heated and unheated cavity walls of the test section are already highly instrumented to measure surface temperature distributions. By virtue of the heater power control system, the heat flux distribution on the heated wall will also be known. Finally, the test section is heavily insulated, so the unheated channel wall will essentially be adiabatic.

Aside from the channel walls, accurate knowledge of the RCCS standpipe surface temperature distributions is equally important, since this information feeds directly into the evaluation of the local heat transfer coefficients, which is key information for code verification and validation. As shown in Fig. 8, the central standpipe will be extensively

instrumented to measure both the inner and outer surface temperatures on surfaces facing both the heated and unheated channel walls. In addition, multi-junction thermocouple assemblies are used to measure axial water temperature distributions in both the downcomer and annular return regions of the standpipe. Furthermore, heat flux meters will be installed to provide local measurements of heat flux through the pipe walls. This information, in conjunction with surface and bulk water temperature measurements, will provide the necessary information for evaluating radial and axial heat transfer coefficient variations within the standpipe.

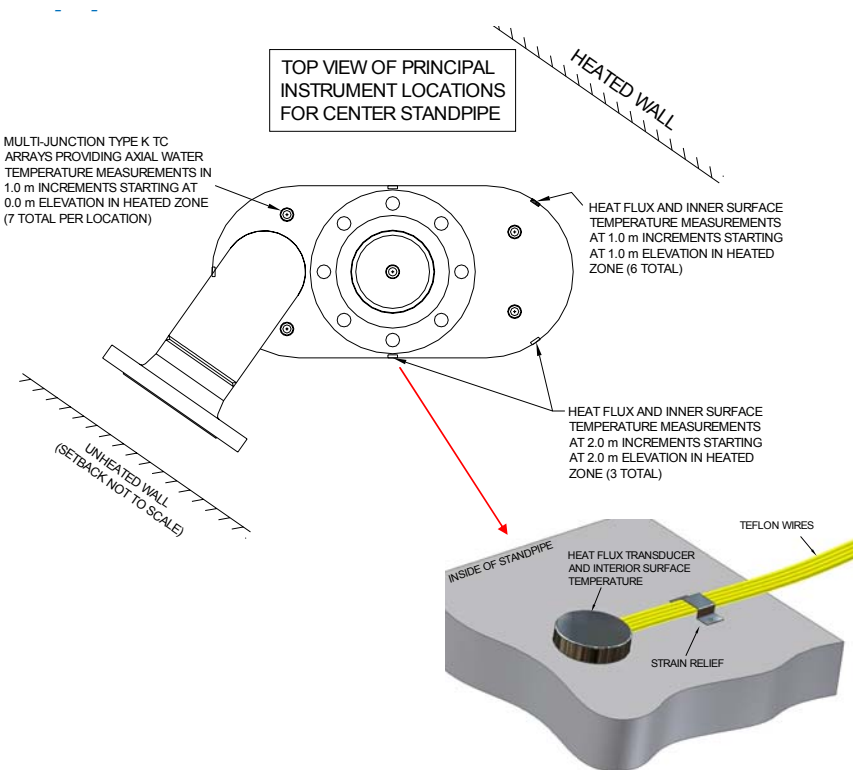

Fig. 8. Center Standpipe Instrumentation Layout

As shown in Table 4, the fourth data requirement is to obtain data on the nature and extent of voiding within the return piping run from the standpipes to the header tank. Differential pressure measurements will be taken at various locations along the pipe in order to estimate local void fractions using well-known techniques. Finally, the onset and extent of boiling within the system is influenced by the local saturation temperature. Given that the system is ~ ½ scale in height, then the saturation temperature in the standpipes may be reduced by as much as 20 ˚C due to the differences in hydrostatic head between the experiment and prototype. On this basis, the system also includes a pressure regulator valve on the outlet to the header tank so that the system pressure can be raised to achieve prototypic absolute pressure within the standpipes if the need arises.

Aside from these instruments that are intended to provide detailed data on the heat transfer behavior within the RCCS standpipes and surrounding structure, other instruments will be provided in order to measure overall system performance and perform heat balances to verify that the system and equipment are functioning properly. For tests

that are intended to investigate system performance under normal forced flow conditions, thermocouples (i.e., RTDs) will be used to measure temperature rise across the standpipes, and temperature loss across the chiller that serves as the ultimate heat sink. Key instrument locations and system setup for the normal operating mode tests are shown in Fig. 9. Overall water flowrate through the system, as well as flowrate through each individual standpipe, will be measured. This information, as well as the input power to the heaters and the temperature changes measured across the standpipes and chiller, will allow energy balance checks to be performed, and to evaluate overall system thermodynamic performance.

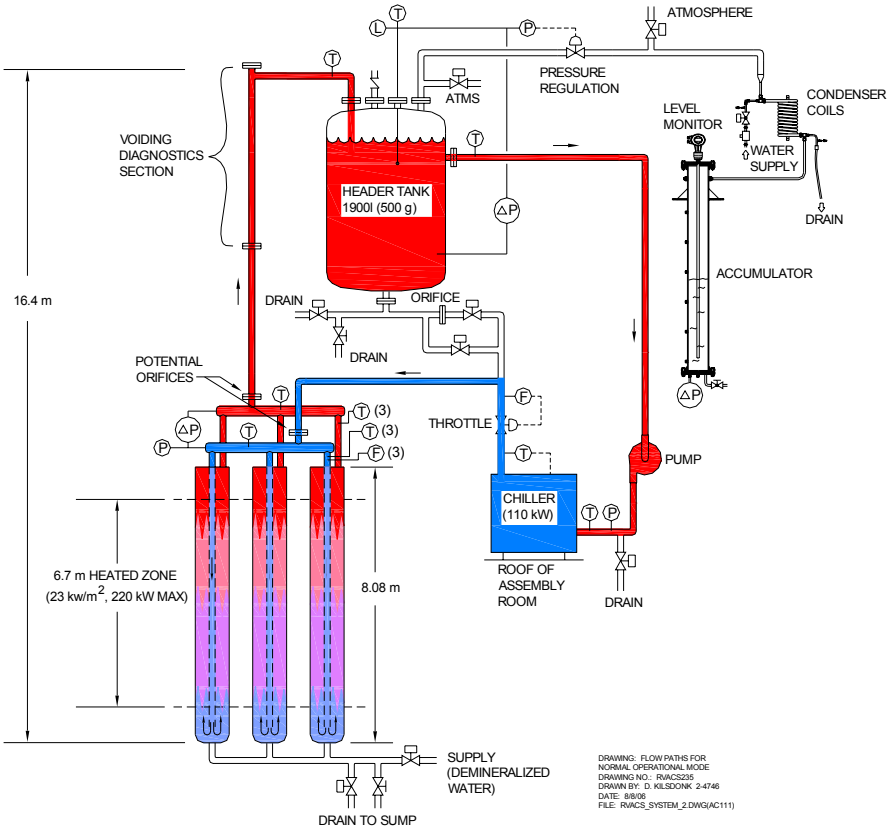

Fig. 9. System Setup for Normal Operations Tests

Instrument locations and system setup for the passive mode tests are shown in Fig. 9. As is evident, for these tests the chiller is isolated and the water supply flowpath is through the orificed supply line located at the bottom of the header tank to the standpipes, whereas the return line is the same as that used for normal operations. In this case, basically all the same measurements will be made as for the full power case, but data gathering will be augmented by collecting and condensing steam that passes through the header tank after saturated conditions are reached, and void fraction distribution along the return line will also be determined. This additional information will help quantify system performance during passive system operation, and augment the database for code validation.

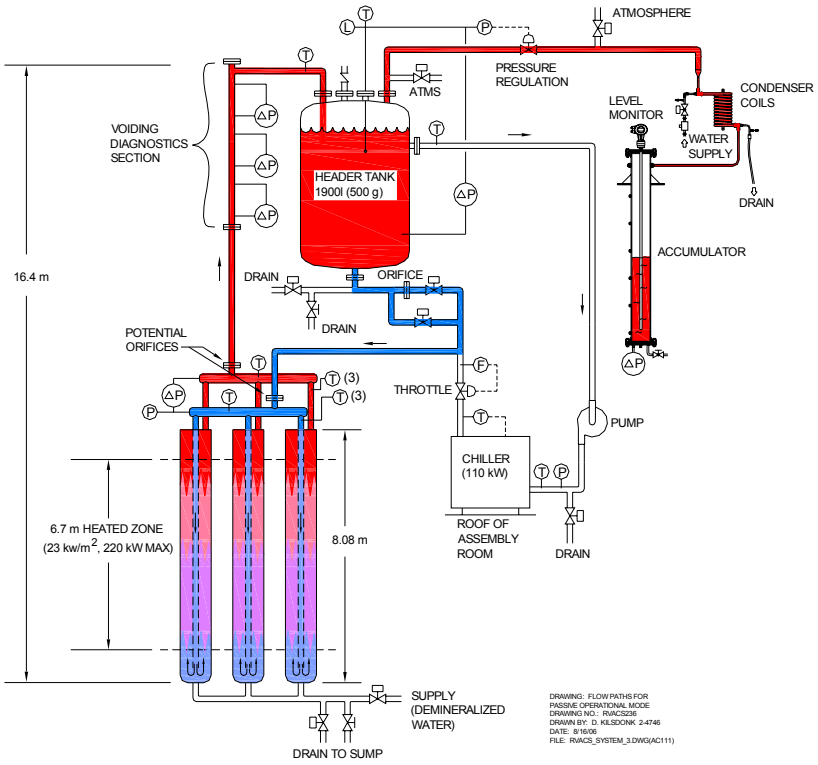

Fig. 10. System Setup for Passive Mode Operational Tests

References

1. R. V. Vilim and E. E. Feldman, "Scalability of the Natural Convection Shutdown Heat Removal Test Facility (NSTF) Data to VHTR/NGNP RCCS Designs", ANL-GenIV-049, Argonne National Laboratory Report, June 2005.
2. C. Tzanos, "CFD Analysis for the Applicability of the Natural Convection Shutdown Heat Removal test Facility (NSTF) for the simulation of the VHTR RCCS", ANL-GenIV-055, Argonne National Laboratory Report, September 2005.
3. M. T. Farmer, et. al., "Natural Convection Shutdown Heat Removal Test Facility (NSTF) Evaluation for Generating Additional Reactor Cavity Cooling System (RCCS) Data", ANL-GenIV-058, Argonne National Laboratory Report, September 2005.
4. M. P. Van Staden, "Analysis of Effectiveness of Cavity Cooling System", Proceedings of the HTR2004 Conference, Paper 20, Beijing, China, September 2004.
5. J.G. Collier, "Convective Boiling and Condensation," McGraw-Hill, NY (1972).
6. A. Manera, H. M. Prasser, and T.H.J.J. van der Hagen, "Suitability of Drift-Flux Models, Void Fraction Evolution and 3D Flow Pattern Visualization During Stationary and Transient Flashing Flow in a Vertical Pipe," The 10th International Topical Meeting on Nuclear Reactor Thermal Hydraulics (NURETH-10) Seoul, Korea, October 5-9, 2003.
7. Thermal-hydraulic Relationships for Advanced Water Cooled Reactors, IAEA-TECDOC-1203, 2001.
8. M. Ishii, et. al., "Modular and Full Size Simplified Boiling Water Reactor Design with Fully Passive Safety Systems," PU/NE-00-17, Purdue University, Annual Report (August, 1999 – July, 2000).
9. R.K. MacGregor, and A.F. Emery, "Free Convection Through Vertical Plane Layers – Moderate and High Prandtl Number Fluids", ASME Journal of Heat Transfer, Vol. 91, pp. 391-403, 1969.
10. F.S. Lien, W.L. Chen, and M.A. Leschziner, "Low-Reynolds–Number Eddy-Viscosity Modeling Based on Non-Linear Stress-Strain/Vorticity Relations", Proc. 3rd Symposium on Engineering Turbulence Modelling and Measurements, Crete, Greece, 1996.
11. T.J. Craft, B.E. Launder, and K. Suga, "Extending the Applicability of Eddy Viscosity Models Through the Use of Deformation Invariants and Non-linear Elements". Proc. 5th International Symposium on Refined Flow Modeling and Turbulence Measurements", pp. 125-132, 1993.
12. A. Durbin, "Separated Flow Computations with the k-e-v2 Model", AIAA Journal, 33(4), pp. 659-664, 1995.
13. C. P. Tzanos, "Heat Transfer Predictions of k-e Turbulence Models in Buoyant Flows", Trans. Am. Nucl. Soc., 88, 239(2003).
14. M. T. Farmer, D. J. Kilsdonk, C. P. Tzanos, S. Lomperski, and R. W. Aeschlimann, "NSTF Facilities Plan for Water-Cooled VHTR RCCS Normal Operational Tests", ANL-Gen IV-080, September 2006.

Nuclear Engineering Division
Argonne National Laboratory
9700 South Cass Avenue, Bldg. 208
Argonne, IL 60439-4842

www.anl.gov

UChicago ▶ Argonne LLC

A U.S. Department of Energy laboratory
managed by UChicago Argonne, LLC